Design and analysis of slider and suspension in 4×1 near-field probe array

Eo-Jin Hong†, Woo-Seok Oh***, Min-Su Jung*, No-Cheol Park**, Hyun-Seok Yang**, Young-Pil Park**, Sung-Q Lee*** and Kang-Ho Park***

Key Words : near-field probe array, optical slider, suspension, shock simulation

ABSTRACT

A lot of information storage devices have been introduced and developed for recently years. The trends of those devices are high capacity, compact size, low power consumption, reliability, and removability for data interchange with other device. As a satisfaction of these trends, near-field technique is in the spotlight as the next generation device. In order for a near-field recording to be successfully implemented in the storage device, a slider and suspension is introduced as actuating mechanism. The optical slider is designed considering near-filed optics. Suspension is not only supports slider performance, and tracking servo capacity but also meets the optical characteristics such as tilt aberration, and guarantee to satisfy shock performances for the mobility for the actuator. In this study, the optical slider and the suspension for near-field probe array are designed and analyzed considering dynamic performance of head-gimbal assembly and shock simulation..

1. Introduction

Near-field optical recording with an optical fiber tip has been considered as a means of increasing recording density. When a beam spot is focused on a near-field aperture, it is possible to record <100 nm data bits [1]. However, low optical throughput on the aperture limits high- speed recording due to low optical intensity. For the satisfaction near-field scanning micro scope (NSOM) technique successfully, many different types of read/write mechanism have been studied in the literature. For the near-field probe array recording, a slider and suspension is introduced. A slider and suspension system is good for stable low flying height and is well verified in conventional hard disk drives actuating mechanism. In order for a near-field to be successfully implemented in the system, a suitable slider and suspension are needed to be properly designed. The optical slider is designed considering near-filed probe optics. The suspension generally supports slider performance, and tracking servo capacity in HDDs. Moreover, the suspension for optical slider also should meet the optical characteristics. Fig. 1 shows the optical and mechanical structure of the near-field probe array. The optical and mechanical structure consists of OFH slider, suspension and optical unit. The laser from the fiber is passed aperture located slider. The slider is connected to actuating system through the suspension-gimbal assembly.

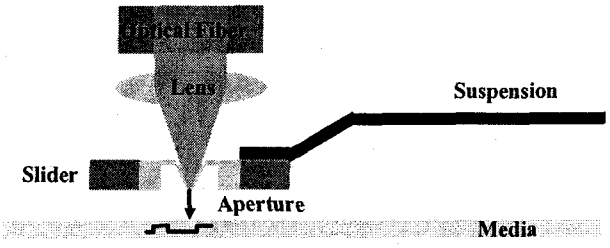

Fig. 1 Optical and mechanical structure of near-field recording

The schematic of probe structure for near-field probe array is introduced as shown Fig. 2. In the cross-section

† Corresponding Author : Storage Systems Division, Semiconductor Business, Samsung Electronics Co. Ltd.
E-mail : hongeojin@yonsei.ac.kr
* Center for Information Storage Device, Yonsei University
** Digital Media Visual, Display Division, Samsung Electronics Co. Ltd.
*** Basic Research Laboratory, Electronics and Telecommunications Research Institute

of the probe structure, the diameter of the prove tip is about 90 nm, and the height of the tip is 7~8 μm. The 4×1 near-field probe array is arranged in the row. The near-field probe array has been fabricated with a SOI wafer using MEMS process [2]. Through the etching process, the shape of the prove tip is made. The layers of the wafer are piled up by Si/SiO2/Si, and the thicknesses of the layers are 10/0.6/500 μm, respectively. The diameter of the probe is 50 μm, and the dimensions of the optical path are 450 μm width, 250 μm length, and 500 μm thickness. The probe array structures included optical path need a bank structure to protect from external particle. The read/write mechanism of the near-field optics demands for the lowest linear velocity considering data transfer rate.

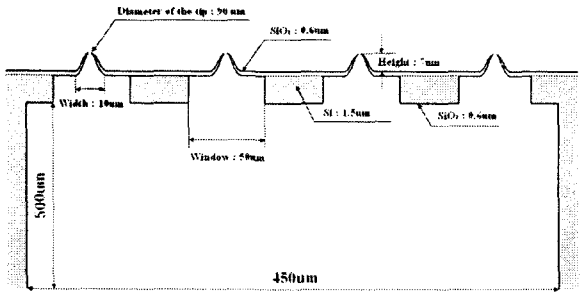

Fig. 2 The scheme of the 4x1 probe array

2. Design of optical slider

For the near-field probe array structure, the slider including bank structure, which protects the probe array, is optically designed. The slider is designed the size of standard nano-slider, and trailing edge part of the slider has rectangular hole for the optical path. A 450 μm×250 μm of bank protects the probe array from particle. Each probe is located 100 μm apart from each other. Fig. 3 shows the SEM image of the near-field probe array. In this figure, the four probes are located in a row. The diameter of probe is 10 μm and its height is 6 μm.

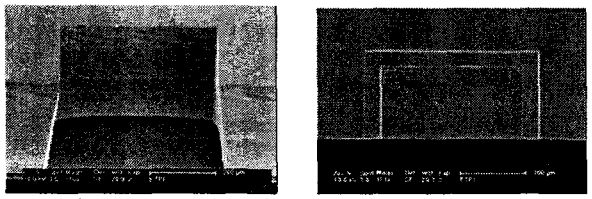

(a) top aspect (b) bottom aspect

Fig. 3 The SEM image of the near-field probe array

The linear disk velocity is fixed on 0.5 m/s, which is minimum velocity that slider is flown stably. The gram load is fixed on 2.5 gf to improve head/disk interface durability. The target flying height between probe and media is about 20 nm. The ratio of flying height modulation to flying height is should be less than 5 %. The pitch angle should be high because high pitch angle improved reliability and performance of a slider. The roll angle should be maintained low because the gap of inner probe and outer probe. And the air bearing stiffness has to high for reliability [3]. The overall dimensions of slider are 2.05 mm×1.6 mm×0.5 mm, which is extended for slider height direction more than standard nano slider that is conventionally used HDDs and gram load is 2.5 gf. Base recess is determined as 6μm because it should be equal height of probe. The front region of slider contains bank structure which protect probe from particle. The surface of slider is flat because mechanical process conventionally used in HDD is not impossible for reason fabrication. Therefore, the camber, crown, taper angle and taper length are ignored.

The design procedure is divided into two steps, propose initial rail design and then, modify the rail design to meet the flying height performance requirement at steady flying state by parameter study. Most modern sliders in HDDs have similar features. In particular area, a recessed area is observed in the center of each slider. This recess creates a sub-ambient pressure zone and a suction force "pulling" the slider towards the disk surface. Towards the leading edge, along the rails of the slider and at the trailing edge pad, raised sections are observed in the slider geometry. These sections create a positive pressure zone and a force "pushing" the slider away from the disk surface.

The combination of the positive and negative air bearing force gives the equilibrium of the slider [4]. Based on these features, two types of initial models are proposed. Fig. 4 shows each type of rail shapes and design parameters. In the indication of slider naming, 'N' means nano slider size, middle name means slider series, and '3C' is denoted that 3 corners bank. The N-01-3C and N-02-3C are symmetric about centerline of the slider. Based on initial models, static analysis is performed to evaluate the flying height performances. The analysis is based on air-bearing simulator.

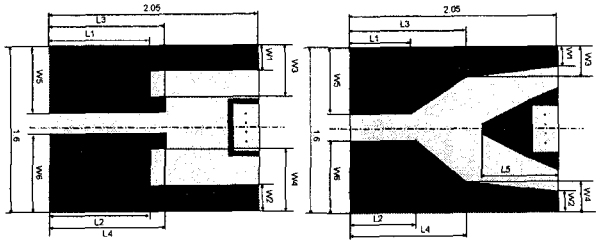

(a) N-01-3C (b) N-02-3C

Fig. 4 Rail shapes and design parameters of sliders

Table.1 Flying height performances of initial model

(a) Static flying height characteristics of initial models

	F. H. [*nm*]	Pitch [*μrad*]	Roll [*μrad*]
N-01-3C	18.92	30.61	-1.72
N-02-3C	19.16	27.80	-1.82

(b) Air bearing stiffness of initial models

	Vertical [*kN/m*]	Pitch [*mN-m/rad*]	Roll [*mN-m/rad*]
N-01-3C	935.80	898.57	30.79
N-02-3C	949.14	965.93	30.01

As shown Table 1, the initial models of slider are listed. The pitch angle is too low and the roll angle is too big, therefore, all two cases of slider designs should be improved. The vertical, pitch and roll air bearing stiffness of N-01-3C and those of N-02-3C also should be modified. By increasing slider's vertical and pitch stiffness simultaneously, decrease flying height modulation and improve flying stability and the ability to follow disk flutter are expected.

Initial rail designs are modified to improve the flying height performance requirements, such as target flying height, high pitch angle, low roll angle and high air bearing stiffness. The parameter study about flying height, pitch angle and roll angle is performed to identify effects that design parameter affect object function. Considering parameter study, the optimal solution is obtained and the tolerance is considered for reliability. Fig. 5 shows final slider models.

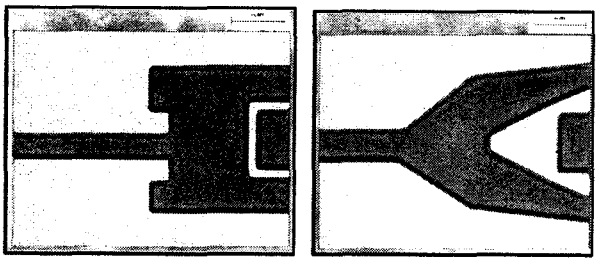

(a) modified N-01-3C (b) modified N-02-3C

Fig. 5 Final slider models

Flying height performance of modified models is listed in Table 2. The flying height of all of two cases is about 19 nm which satisfy the requirement. In case of slider N-01-3C, the pitch angle is increased about 50 % and the roll angle is decreased about 90 % than initial model. In case of slider N-02-3C, the pitch angle is increased about 2 % and the roll angle is decreased about 70 % than initial model. Negative pressure zone near the bank structure of N-01-3C are wider than that of N-02-3C. Generally, negative pressure can keep constant flying height. Thus, N-01-3C has the advantage over N-02-3C in flying height modulation. Higher air bearing pressure leads to higher flying stability and the ability to follow disk flutter. Thus, air bearing pressure is the one of key factors for evaluating performances of slider. As listed in Table 3, the N-01-3C has higher air bearing stiffness values than the N-02-3C. Based on simulation results, the N-01-3C designs provide superior performance in all respects except the roll stiffness, as compared to the N-02-3C design.

Table 2 Flying height performances of modified model

	F.H. [*nm*]	Pitch [*μrad*]	Roll [*μrad*]
N-01-3C	19.04	46.19	-0.19
N-02-3C	19.27	28.25	-0.50

Table 3 Air bearing stiffness of modified model

	Vertical [*kN/m*]	Pitch [*mN-m/rad*]	Roll [*mN-m/rad*]
N-01-3C	1337.76	1220.99	-27.18
N-02-3C	947.42	952.56	60.19

3. Design of suspension

In disk drives, head-suspension is provided which support a read/write head to fly over the surface of the disk when it is rotating. Specially, the optical flying head is typically located on the slider having an aerodynamic design so that the slider flies on an air bearing generated by the rotating disk. In order to stabilize the flying height, the head-suspension is also provided with a spring force counteracting the aerodynamic lift force.

Generally, a head-suspension is hard disk comprises a load beam and a flexure to which the sliders to be located. However, in order to easy manufacturing and high reliability, we imported integrated type suspension. The main target of this suspension for near-field probe is easy available fabrication with stable compliance to the disk. The suspension should be support the slider at the vertical, roll, and pitch direction of its motion. Moreover, the suspension should robust to the track direction. For the satisfaction these targets, this suspension is suggested integrated type, which is applied optimal design methods such as topology and shape optimization.

Fig. 6 shows the scheme of the initial suspension. The features of the suspension are unique flexure part, rib, narrow spring region, topology region and various width of the load beam. The initial mode is obtained by parameter study. As the integrated gimbal part is designed equal to the thickness of the load beam, the

flexibility of gimbal is only controlled by shape function of gimbal structure. Accordingly, the parameter study of gimbal is performed independently. The targets of specification are as follows. The 2nd torsional frequency and sway frequency target higher than 10 kHz in order to guarantee 2 kHz servo bandwidth. The vertical stiffness targets 18~30 N/m, the roll stiffness targets 18~30 μNm/deg and the pitch stiffness targets 2~5 μNm/deg for flying height stability.

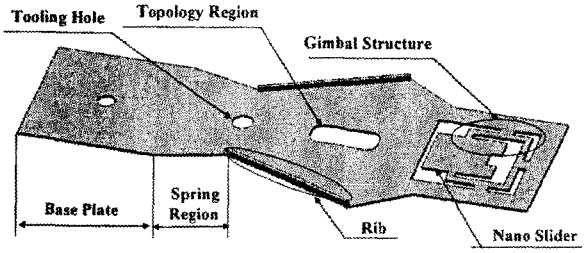

Fig. 6 Initial model of the suspension

Based on constraints, shape optimization is applied with combination of sub problem approximation method first order method. The sub problem approximation method is an advanced zero-order method that can be efficiently applied to most engineering problems. The first order method is based on design sensitivities and is more suitable for problems that require high accuracy. The objective function OBJ is defined as a weighted sum of the second torsional frequency λ_{2T} and the sway frequency λ_S respectively normalized with their initial eigenvalues [5],

$$OBJ = w_{2T}\lambda_{2T} + w_S\lambda_S \quad (1)$$

A nearly equal effort is made to increase the second torsional frequency and sway frequency with $w_{2T} = 0.6$ and $w_S = 0.4$. The objective is to maximize the objective function without any significant changes in other constraints factors. Fig. 7 shows 1st fine model. The shape of spring region is modified and design parameters for gimbal part are stabilized. The rib structure is removed to simplify shape of suspension.

Moreover, topology optimization is performed to reduce effective mass while frequency characteristics are almost same [6]. The weighted mean function is defined as a weighted sum of the natural frequencies. Fig. 8 shows the results of topology optimization. As shown this figure, a bar graph below the analyzed suspension is shown the various pseudo density distributions from 0.0 to 1.0. The density of 1.0 should be kept area, and the density of 0.0 is able to remove without significant effect of characteristics. Based on result of the topology optimization, hole in middle portion of load beam is designed for topology optimization additionally. Low mass is good for compliance and anti-shock performance.

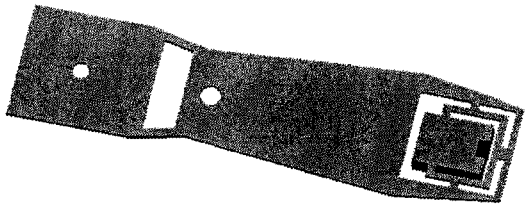

Fig. 7 1st fine model

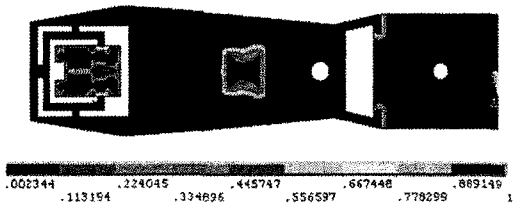

Fig. 8 Results of the topology optimization

To obtain the frequency characteristics of topological model, modal analysis is executed using finite element solver ANSYS. Effective mass is decreased 10 % than 1st fine model while lateral and torsional frequencies are almost same. Fig. 9 shows final model which is fabricated. The 2nd torsion and sway frequency of final model are 8.6 kHz and 13.0 kHz. The vertical, pitch and roll stiffness are 29.6 N/m, 1.6 μNm/deg, and 29.7 μNm/deg.

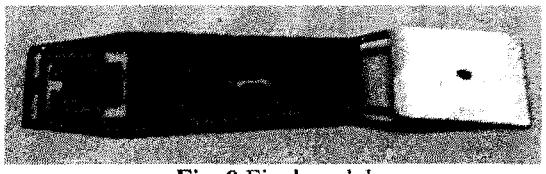

Fig. 9 Final model

4. Dynamic and shock analysis of HGA

For the measurement of the flying height and its variation, the two beams of the LDV are utilized. The one measures the tip of the slider, and another measures the nearest point of the slider on the disk. Fig. 10 shows the experimental setup. It consists of LDVs, disk, air bearing motor, and CCD camera. The gram-load is 2.5 gf, and the linear velocity is 0.5 m/s. Experiment is made in the class 1000 clean room. The two beams of LDVs are measured the flying height and the HGA is fixed at the micro stage. The specification of flying height test are 3.5 inch aluminum disk, 960 rpm rotating speed of disk, skew angle of slider is 0 degree, and radial position of slider is 10mm.

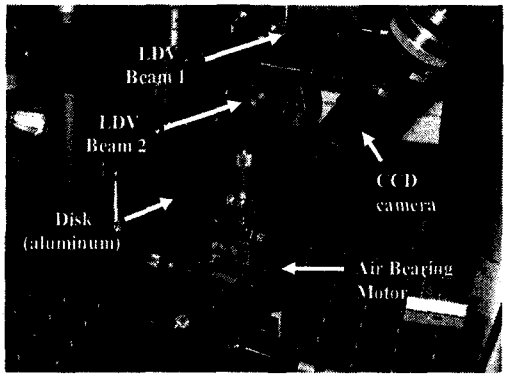

Fig. 10 Experimental setup

Fig. 11 shows results of noise elimination. The noise is calculated with averaging of repetitions test. And RRO component of the disk is filtered with Chebyshev Type I. The resultants show that Model of N-01-3C is about 15 nm fling height, and model of N-02-3C is about 49 nm flying height.

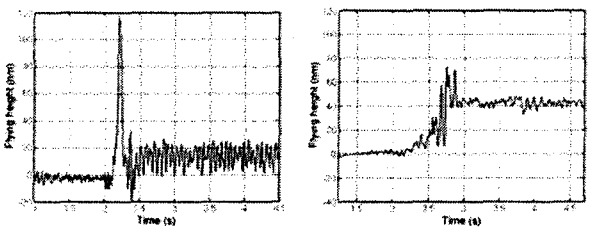

(a) N-01-3C (b) N-02-3C

Fig.11 Results of flying height test

The shock analysis during operational state is performed with ANSYS/LS-DYNA, a nonlinear finite element solver. The finite elements model consists of the optical flying head slider with near field probe array, suspension, and one inch disk. The deck and the swing arm type rotary actuator don't consider because they are relatively robust against external shock impulse. The slider and the disk are constructed as SOLID164 elements. On the other hand, the suspension is constructed as SHELL163 elements. Due to hourglass energy problem, the fully integrated Belytscho-Tsay element formulation was used to shell element. The Flanagan-Belytscho stiffness form of hourglass control with a coefficient of 0.01 is used to minimize hourglass energy for solid element in the model. The model contains 2102 elements and 3422 nodes. Fig. 12 shows finite element model. The operational model is structurally the same as the non-operational model however the operational model must account for the hydrodynamic lubrication, that is, the air bearing between the optical slider and disk during the operating state [6]-[8].

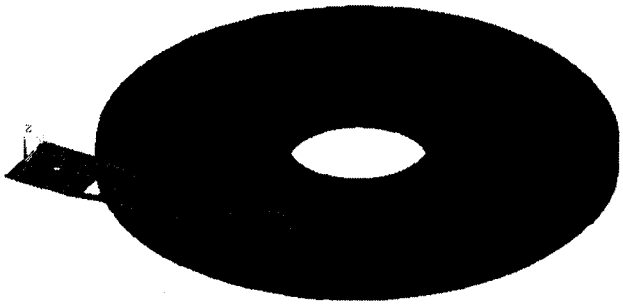

Fig.12 Finite element model of a disk drive

The air bearing effect is assumed the vertical-direction four compressible spring and damper components, which are located the corner of the slider. The total stiffness of the air bearing is calculated 1337 kN/m. The relative stiffness ratio is modeled as $k_{LEI} : k_{TEI} : k_{LEO} : k_{TEO} = 1 : 2.75 : 1.08 : 2.47$. The inner leading edge of the slider is denoted as LEI. Similarly, the inner trailing edge, outer leading edge and outer trailing edge are denoted as TEI, LEO and TEO, respectively. The damping ratio of air bearing is 5%. Shock analysis during operational state is performed from the viewpoint of shock magnitude. The peak magnitude of shock is varied 175 G, 350 G and 700 G. Duration of shock is fixed 0.5 ms in all of three cases. The displacement contour is simulated during the transient response from 0ms to 3ms in all of cases. During a shock analysis, it is interesting points that relative displacement between the bottom of the slider and the top of the disk. The relative displacement during 175 G half sine shock impulse over 0.5 ms is displayed in Fig. 13. The displacement of the leading edge is more variable than that of trailing edge because of air-bearing stiffness of trailing edge is larger than that of leading edge.

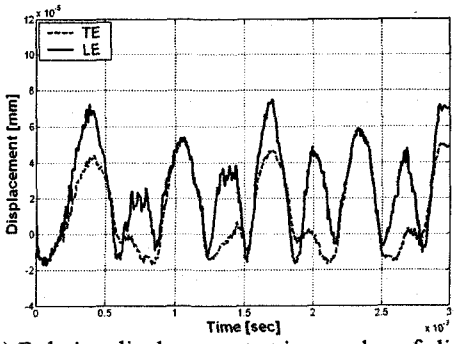

(a) Relative displacement at inner edge of slider

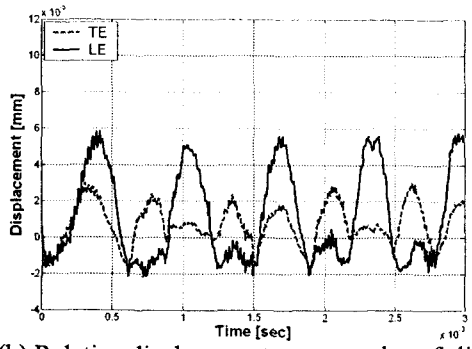

(b) Relative displacement at outer edge of slider

Fig 13 Relative displacements during shock simulation

Table 4 the results of simulations are listed. The displacement of the PC disk is more variable than that of glass disk. Through shock analysis of operating state, it is confirmed that the air bearing effect is dominant factor. The results from the simulations provide insight into the characteristics for both operational and non-operational disk drive and are useful to design disk drive design to withstand shock.

Table 4 Shock responses of PC and Glass disk

			175G		350G		700G	
			PC	Glass	PC	Glass	PC	Glass
Relative displacement [nm]	IE	LE	75	178	199	502	357	1067
		TE	59	106	94	282	191	607
	OE	LE	58	149	193	454	352	924
		TE	30	89	89	210	152	486
Pitch [mrad]	IE		0.07	0.04	0.28	0.12	0.34	0.25
	OE		0.07	0.03	0.29	0.12	0.35	0.25
Roll [mrad]	LE		11.01	1.03	35.74	2.06	71.92	4.15
	TE		11.01	1.02	35.74	2.05	71.95	4.12
Contact Force [N]			0.12	0.16	0.22	0.30	0.38	0.64

5. Conclusion

We designed optical slider and integrated suspension for 4×1 probe array. For slider, two initial model of the slider are proposed. The trailing edge of slider contains bank structure which protect probe from particle. The slider models are modified by using parameter study and flying performances of the models are compared to meet the flying performances requirement. The flying height, pitch angle, and roll angle are 19.04 nm, 46.19 μrad and -0.19 μrad. The vertical and pitch stiffness of air bearing are 1337.76 kN/m and 1220.99 mN-m/rad. For suspension, integrated type suspension is adapted. Based on parameter study and topological optimization, initial model is modified. Effective mass is decrease about 10% than initial model. The 2nd torsion and sway frequency of final model are 8.85 kHz and 13.01 kHz. The vertical, pitch and roll stiffness are 29.58 N/m, 1.64 μNm/deg, and 29.66 μNm/deg. Moreover, the HGA of near-field recording is experimented for flying height and is simulated for shock response with ANSYS/LS-DYNA. This actuating system will be realized for 1 TB data storage recording.

Acknowledgement

This work was funded by the Korea Science and Engineering Foundation (KOSEF) through the Center for Information Storage Device (CISD) Grant No. R11-1997-042-11001-0.

Reference

(1) K. Song, E. Kim, S. Lee, J. Kim, and K. Park, "Fabrication of a high-throughput cantilever-style aperture tip by the use of the bird's-beak effect", Jpn. J. Appl. Phys. Vol. 42, 2003, pp. 4353–4356

(2) E. Kim, S. Lee, and K. Park, "Fabrication of a near-field arrayed for the optical data storage", International Symposium on Optical Memory, 2004, pp. 136-137

(3) Lu S. and Bogy D. B., 1996, "Air Bearing Design, Optimization, Stability Analysis and Verification for Sub-25nm Flying," IEEE Trans. Magn., Vol. 32, pp. 103-109.

(4) Dufresne M. A. and Menon A. K., 2000, "Ultra-Low Flying Height Air Bearing Designs", IEEE Trans. Magn., vol. 36, pp. 2733-2735.

(5) Gih Keong Lau, Hejun Du, and Ling Pan, 1997, "Optimal design of suspension for high-density magnetic recording systems", IEEE Trans. Magn., Vol. 38, pp. 2165-2167.

(6) Jasbir S. Arora, 2001, "Introduction to optimum design", McGraw-Hill, New York, USA

(7) Eric M. Jayson, James M. Murphy, Paul W. Smith and Frank E. Talke, 2002, "Shock and head slap simulations of operational and nonoperational hard disk drives", IEEE transactions of magnetics, Vol. 38, No5, September

(8) Eric M. Jayson, Paul W. Smith and Frank E. Talke, 2003, "Shock modeling of the head-media interface in operational hard disk drive", IEEE transactions of magnetics, Vol. 39, No5, September